ELSEVIER

Wear 195 (1996) 223–231

WEAR

Whisker behaviors and tool wear in cutting of unidirectional SiC whisker-reinforced plastic

J.E.D. Afaghani [a], K. Yamaguchi [a], I. Horaguchi [b], T. Nakamoto [a]

[a] *Department of Mechanical Engineering, Nagoya University, Furo-cho, Chikusa-ku, Nagoya 464, Japan*

[b] *Toyota College of Technology, Eisei-cho 2-1, Toyota-shi, Aichi, Japan*

Received 14 November 1995; accepted 8 February 1996

Abstract

This study concerns the cutting process of unidirectional SiC whisker-reinforced plastic composite. The effects of the grain size of the polycrystalline diamond tool and the SiC whisker orientation on the tool wear were investigated.

The tool with fine grain size exhibited higher wear rates. The greatest tool wear was with the composite having longitudinal alignment of whiskers. The cutting processes of various orientations of whiskers were observed by scanning electron microscopy at low speed using a specially designed device. Moreover, models were proposed for cutting the SiC whisker–plastic composite and for wear of sintered diamond tools.

Keywords: Cutting; Silicon carbide whisker; Orientation; Plastic composite; Polycrystalline diamond; Grain size; Tool

1. Introduction

In the last decade, fibers made of silicon carbide, aluminum oxide and silicon nitride have been widely used as reinforcement in composite materials, mainly because of their high mechanical properties and fairly low density, which are the potential demands in the manufacturing of airplane and aerospace shuttle parts.

SiC whisker is characterized by its unique mechanical properties. It has a tensile strength and Vickers hardness of up to 14 GPa and 80 GPa, respectively.

SiC whiskers have been applied mostly as reinforcement in metals and ceramics [1–6]. Some researchers [7–10] have checked the improvement of mechanical properties and wear resistance when SiC whisker–aluminum composites are used. Other investigations [11–20] have been carried out on the application of SiC whiskers to ceramics cutting tools where the inclusion of whiskers could improve the tool toughness, wear resistance and thermal shock resistance. Xiao et al. [21,22] studied the effect of whisker orientation on the wear resistance and cutting performance of whisker–ceramic tools.

Only a few researchers considered the application of SiC whiskers to plastics [23–25], since whisker–plastic composites are too expensive to come into industrial application. Zhang and coworkers [23] showed that SiC whiskers could improve the flexural modulus of epoxy slightly more than that of continuous glass fibers. Although SiC whiskers are very short, fine fibers and rather expensive, SiC whisker–plastic composites can be applied to micro-machine elements, which have been attracting the attention of researchers in the bio, medical and informatic engineering fields. The mechanical properties of micro-size plastic elements can greatly be improved by the inclusion of SiC whiskers.

Machining of composite materials is required to obtain the desired size and surface finish of composite parts. While the mechanical properties of plastics are improved by the inclusion of SiC whiskers, the cutting of these composites, however, becomes more difficult. Cutting tools suffer from the abrading action of whiskers.

This paper deals with the cutting of SiC whisker–plastic composites. The attempt was made to analyze the cutting process. The effect of the orientation of SiC whiskers in the composite on the tool wear was investigated. The grain-size factor of sintered diamond tools was conducted in the analysis of tool wear mechanisms in cutting of unidirectional SiC whisker-reinforced plastic. Moreover, the authors attempted to simulate the cutting process at low speed by scanning electron microscopy (SEM) direct observation and established appropriate cutting models. Another approach model

PII S0043-1648(96)06953-0

has been introduced to determine the effect of microstructure of sintered tool and whisker size on the breakage of tool grains.

2. Experimental program

Polycrystalline sintered diamond tools were used in the cutting experiments. Two types of different grain sizes were selected, fine grain size of $d = 0.5$ μm and coarse grain size of $d = 5$ μm. Table 1 shows some characteristics of the tools. Fig. 1 shows scanning electron micrographs of fine and coarse grains of sintered diamond tool materials.

Cutting experiments were performed on a lathe equipped with a smooth-variable-speed controller to allow a constant cutting speed with changes of the specimen diameter. The cutting conditions are shown in Table 2. For each experimental set, three similar experiments were repeated and the mean values were considered in the results.

The wear micrography was observed by SEM. Tool wear was evaluated by flank wear width, which was measured by optical microscope accessed with digital x–y table of 1 μm accuracy.

The composite used consists of epoxy resin as matrix and SiC whiskers as reinforcement. The volume content of SiC whisker was 14%. Table 3 illustrates the characteristics of the composite's components. Unidirectional SiC whisker–plastic was prepared according to the method of Yamaguchi and Horaguchi [25]. The specimens for cutting experiments were of cylindrical shape ∅30 × 50 mm. Three types of specimens have been employed in this work. The classification was made according to the whisker orientation against the

Table 1
Polycrystalline sintered diamond inserts

Tool code	Grain size d (μm)	Hardness HV (GPa)	TRS [a] (GPa)	Rake/clearance angles	Nose radius (mm)
PCDF	0.5	≈ 100	2.2	5°/6°	0.2
PCDC	5	≈ 120	2.0		

[a] Transverse rupture strength.

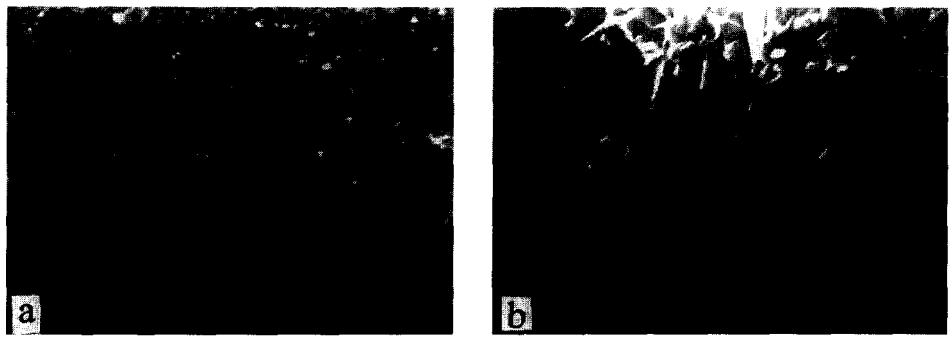

Fig. 1. Scanning electron micrographs of sintered diamond tool materials: (a) fine grain ($d = 0.5$ μm); (b) coarse grain ($d = 5$ μm).

Table 2
Cutting conditions

Cutting speed V (m min^{-1})	Depth of cut t (mm)	Feed rate f (mm rev^{-1})	Coolant
100	0.5	0.025	Dry

Table 3
Characteristics of the components of the composite

Component	Matrix	Reinforcement
Maker	Araldite®, CIBA–GEIGY (Swiss)	TOKAMAX-SiC, TOKAI CARBON (Japan)
Composition	Resin: AW106 (1 vol.) Hardener: HV953U (1 vol.)	β-SiC
Dimension	–	∅1 × 50 μm
Density	1.07×10^3 kg m^{-3}	3.2×10^3 kg m^{-3}
Tensile strength	≈ 18 MPa	3–14 GPa
Vickers hardness	≈ 30 MPa	≈ 80 GPa
Mixing percentage	86 vol.%	14 vol.%

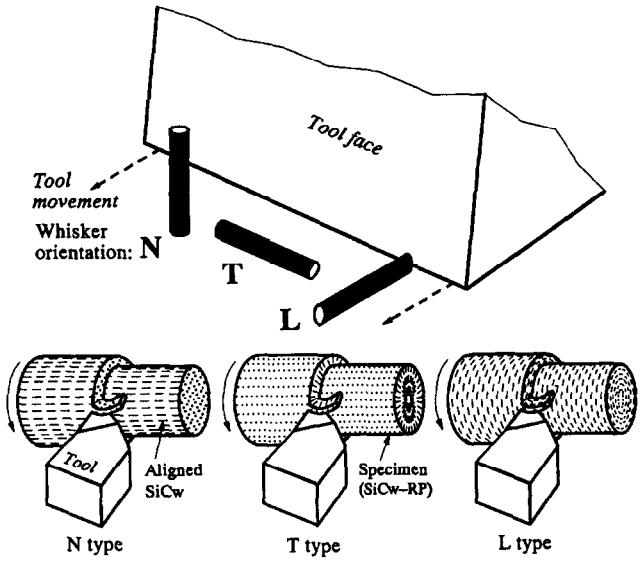

Fig. 2. Cutting set-up of three types of the composite.

Fig. 3. Scanning electron micrograph of unidirectional SiC whisker–plastic composite.

cutting direction. They are designated as longitudinal (L), normal (N) and transversal (T) types. Fig. 2 illustrates the set-up of the cutting experiments with the different whisker alignments. Fig. 3 shows a scanning electron micrograph of the unidirectional SiC whisker–plastic composite.

Since the concerned composite in this paper has not been previously studied, the authors herewith provide an introduction to some of its mechanical properties. Simple tensile tests

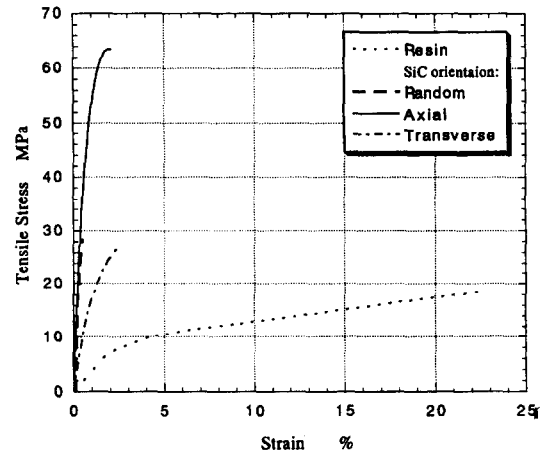

Fig. 4. Tensile tests of the resin and the composite.

have been done on a plate-shape test piece of 4×8 mm^2 cross-section. Tests have been carried out for random, axial and transverse orientations of whiskers, and compared with the data of epoxy resin. Fig. 4 illustrates the nominal stresses against the strain for all tested types. Whiskers have apparently increased the tensile strength and the rigidity, but decreased the toughness of the epoxy resin. Moreover, aligning whiskers in the axial direction results in the highest improvement of tensile strength; for instance, three folds of the epoxy resin strength could be obtained. Table 4 lists some mechanical properties of the tested composite and resin.

3. Results and discussions

3.1. Wear and cutting forces

Two types of polycrystalline sintered diamond tools ($d = 0.5$, 5 μm) have been employed in the cutting experiments. Fig. 5 compares the flank wear widths V_B of both tools for L, N and T types of composite. The greater flank wear widths were found in the fine grain tools. Moreover, in both tools, the greatest wear rates were with the L type composite among the three types.

Table 4
Mechanical properties of the tested composite and resin

Property	Epoxy AW106:HV953U	Composite type		
		Random	Axial	Transverse
Tensile strength (MPa)	18	28	64	28
Young's modulus (GPa)	0.5	3.5	10.5	2.5
Elongation (%)	22.5	0.4	2.1	2.7
Vickers hardness (MPa) †	30	150	165 [a)]–230 [b)]	
Density (kg m^{-3})	1.07×10^3	1.36×10^3		

†

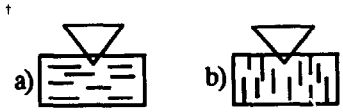

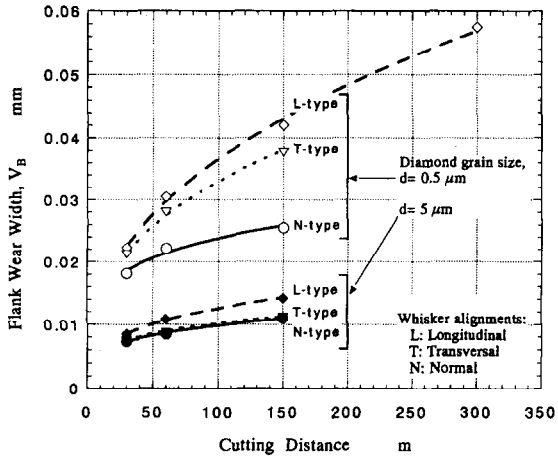

Fig. 5. Flank wear widths of sintered diamond tools for three types of composite.

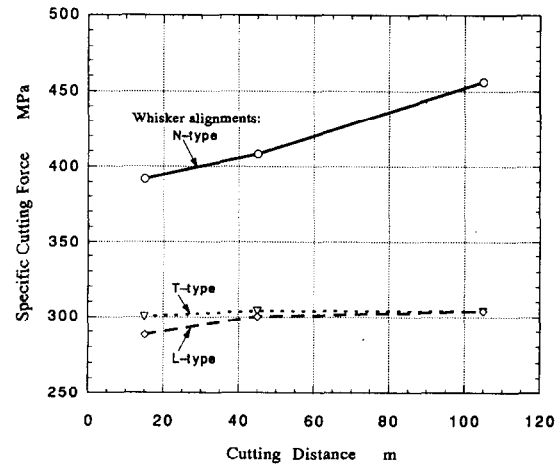

Fig. 7. Specific cutting forces of three types of composite cut by fine-grain sintered diamond tool.

SEM of the worn tool edges shows that the wear volume of the fine grain tool is greater than that of the coarse one as illustrated in Fig. 6. Worn edge of the fine grain tool looks smoother than that of coarser one. Micro-chippings of the grain size are observed on the edge. The primary reason for these differences is the grain size. The coarser diamond grains ($d=5$ μm) in the sintered diamond tool could resist the severe plucking action of SiC whisker (∅1 μm) more effectively.

Fig. 7 shows the specific cutting forces of the fine grain diamond tool in relation to cutting distance for L, N, and T types of composite. The N type composite exhibits the greatest specific cutting force. However, the cutting forces of L and T type are almost identical.

It is worth noticing that L type had the highest wear rate but a lower cutting force. Whereas the opposite results have been obtained with N type composite.

3.2. *Cutting process under SEM observation*

A special device has been designed and made to perform the cutting at very low speed inside the scanning electron microscope chamber to allow observation of the cutting process.

Fig. 8 demonstrates the cutting process of N type composite. We can distinguish the deformation zones where initial cracks exist in the matrix from the tool edge to the cutting direction, mostly with a down-slope (Fig. 8(a)). The whisker tends to be pulled out from its matrix, then abrades the tool edge (Fig. 8(b)). The chip formation is much harder than other types, since the whiskers here resist more the crack propagation in composite in the cutting direction. Moreover, deformation of the matrix below the tool edge is high in comparison with other types. The tool edge bends the whiskers that may be broken out or elastically bent. For instance, in Fig. 8(b), a micrograph of broken whisker is shown. The chip formation here is considered "tear type".

Cutting of T type composite is demonstrated in Fig. 9. The observation of the process shows that by the tool edge movement, a deformed zone of the composite exists and flows along a shear plane; thereafter, cracks initiate in the matrix from the tool edge side with the shear direction and the deformed material slides with the crack direction for a while, then a new deformation zone is generated again in the next location. The cutting mechanism here is rather similar to the shear plane model with discontinued chip formation that can be referred to as "shear type".

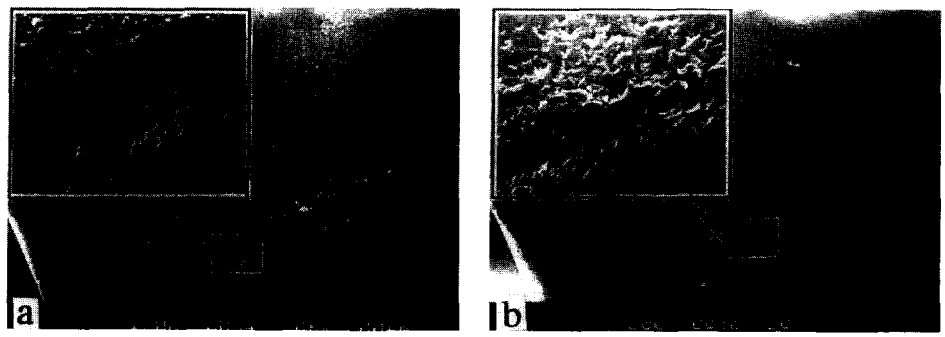

Fig. 6. Scanning electron micrographs of worn edges of fine and coarse grains: (a) fine-grain sintered diamond tool; (b) coarse-grain sintered diamond tool. (Cutting distance = 150 m; workpiece: L type composite.)

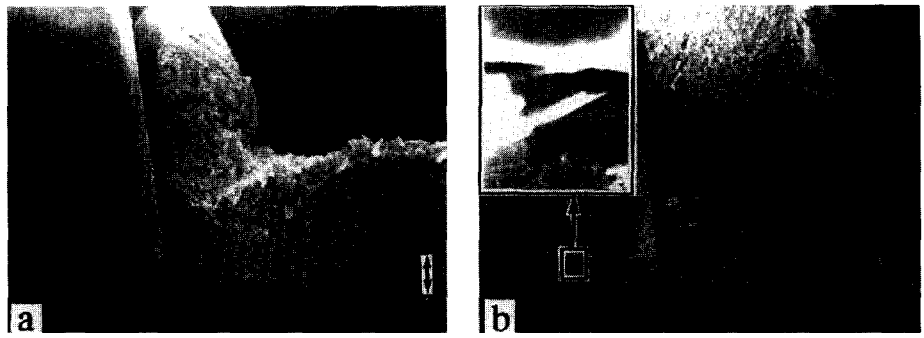

Fig. 8. SEM observation of cutting N type composite: (a) $t=30$ μm; (b) $t=80$ μm.

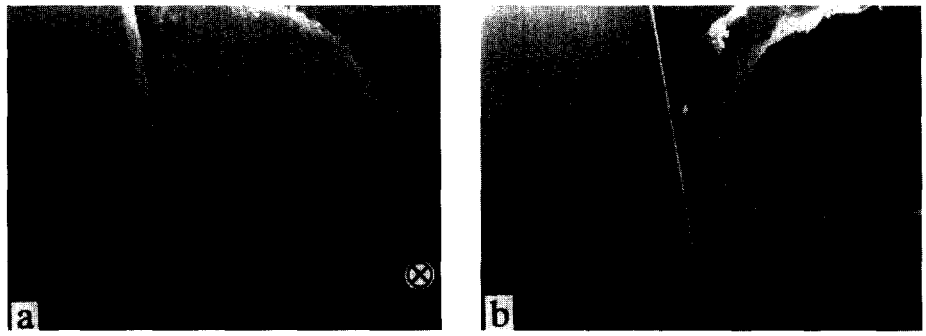

Fig. 9. Typical scanning electron micrographs while cutting T type composite ($t=80$ μm): (a) deformation zone; (b) chip shape.

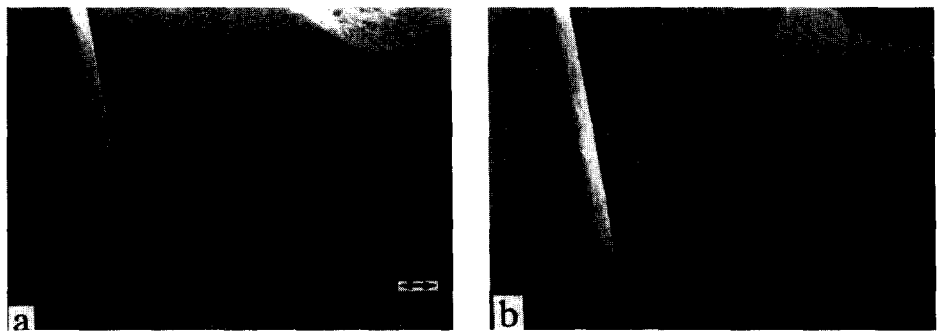

Fig. 10. Sequential scanning electron micrographs of cutting L type composite ($t=110$ μm): (a) crack propagation; (b) chip flow.

Fig. 10 shows sequential micrographs of cutting L type composite. In the tool edge movement, a crack initiates in the matrix from the tool edge side and propagates to the cutting direction. The direction of whiskers here facilitates the crack generation so as to be parallel to the tool movement, but it prevents the formation of shear plane, as a result, chip is bent and flows along rake face (Fig. 10(b)). The chip looks like "flow type". The matrix deformation below the tool edge is low owing to the straight crack generation. From the observation of whisker behavior against the edge tool, a whisker may escape inside the cut matrix below the tool edge, or be pushed forward; bent and broken out, or be torn with the chip from the composite and slide along the tool rake surface.

The actual cutting process at ordinary cutting speed may be different from the SEM observations. However, no changes are expected in fundamental of chip deformation and mechanisms such as fracture or debonding of whiskers.

4. Cutting models and analysis

Cutting models have been made to illustrate the wear mechanisms of tools with different grain sizes and different orientations of whiskers. Moreover, a model of grain tear-off in tool edge is introduced to explain the weakness of fine grain edge against the aligned whiskers in the longitudinal direction.

4.1. Cutting models

The cutting experiments and the cutting observation by SEM lead to build up the cutting models of SiC whisker–plastic composite with sintered diamond tools. Fig. 11 illustrates the cutting model of N type composite with fine grain tool. The model shows that by tool edge movement, a crack generates in the deformation zone and propagates down-

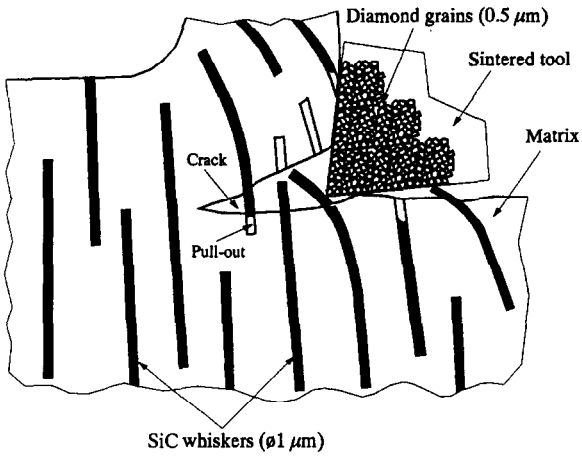

Fig. 11. Cutting model of N type composite with fine-grain sintered diamond tool.

wards. Some whiskers are pulled out and flow with the cut chip. Others, with longer roots, remain in the work material with their top parts protrude from the cut surface; then the tool edge bends the top parts of these whiskers, which may be broken out or escape under the tool edge with matrix deformation. As the whisker diameter is very small, bending of SiC whiskers in N type does not require high pressure by the tool edge. However, the mean force to cut N type composite is expected to be greater than those of other types because the tool edge should overcome extra forces to pull whiskers out from the matrix with the generation of the crack and whisker resistance of chip deformation in the shear zone. The wear of tool and cutting force introduced in Fig. 5 and Fig. 7 are consistent with this model.

Fig. 12(a) demonstrates the ideal cutting model of T type composite. When the tool cuts this composite, whiskers contact the tool with their cylindrical surfaces since they are parallel to the tool edge. Moreover, the whiskers allow the generation of a shear plane, so a low cutting force is expected. For perfect whisker orientation, the tool edge contacts the whole length of whisker at once (Fig. 12(b)). Therefore, the stress concentration on a grain is not relatively high. Hence, the tool wear is expected to be lower than in cutting composites of other orientations. This prediction does not match that of the wear experiments for the following reasons. The T type composite is very sensitive to disorientation as illustrated in Fig. 12(b). A slight inclination of whiskers can not be avoided when fabricating the workpieces. This causes the breakage of some whiskers and partial debonding of some others when the tool edge passes through these whiskers. Fig. 12(c) shows a scanning electron micrograph of the cut surface, which indicates the broken and partially debonded whiskers. Moreover, whisker inclination produces a higher stress concentration compared with that of the ideal model. The last factor leads to the higher tool wear than the expected one.

Fig. 13 demonstrates the cutting model of L type composite with fine grain tool. Whisker with L orientation resists the generation of shear plane, but facilitates the crack to propagate parallel to whisker axis. In this case, whisker end collide with the diamond grain and exerts high local stress on the tool edge because it is supported behind by the entire cylindrical bonded surface. This can not exist in the other orientation types, so the highest wear rate of tool edge is predicted with L type composite by the active tear-off mechanism. The experimental work has shown that L type has the most severe tool wear (refer to Fig. 5).

Taking into consideration the grain size of the tools, the larger grains are predicted to resist better the tear-off mechanism in the wear of sintered tools. Fig. 14 illustrates the

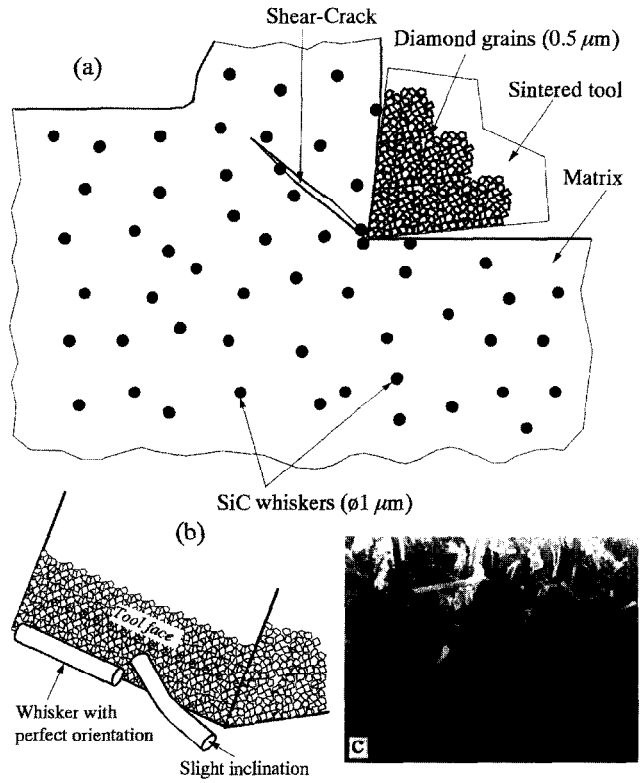

Fig. 12. Cutting model of T type composite with fine-grain sintered diamond tool: (a) ideal cutting model; (b) changes in cutting mechanisms by whisker inclination; (c) scanning electron micrograph of the cut surface.

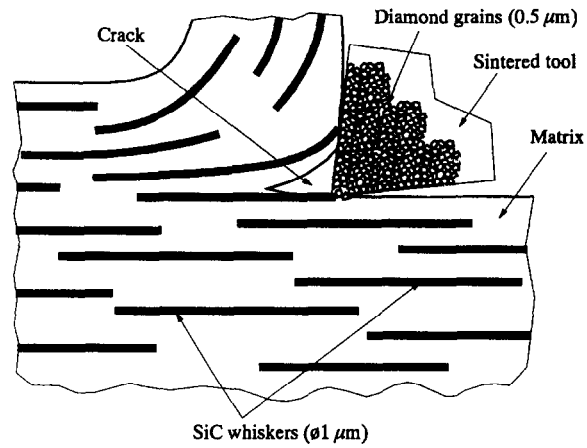

Fig. 13. Cutting model of L type composite with fine-grain sintered diamond tool.

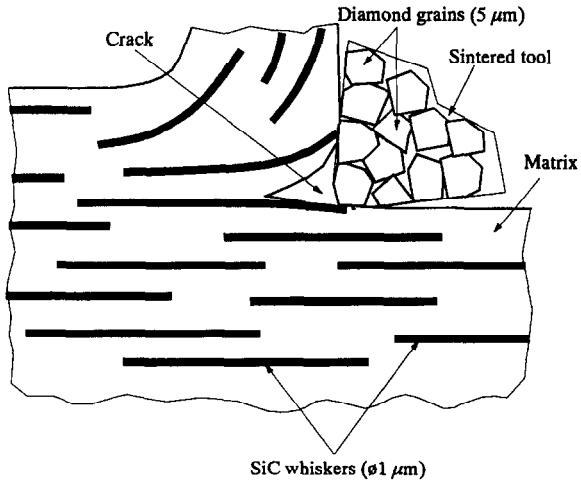

Fig. 14. Cutting model of L type composite with coarse-grain sintered diamond tool.

cutting model of L type composite with coarse grain tool. Comparing Fig. 13 and Fig. 14, the tear-off force for one coarse grain is apparently much greater than that of a fine one owing to the larger bonding surface. Therefore, in order to tear off the coarse grain, it requires many more collisions by whiskers to reach the fatigue strength of the bonding material. This leads to a lower wear rate of coarse grain tool in cutting SiC whisker–plastic composite, which can explain the experimental results in Fig. 5.

4.2. *Whisker–tool interaction analysis*

Analytical model has been established to demonstrate mathematically the tear-off mechanism of grains of sintered tools. The calculation helps to determine the effects of tool grain and whisker sizes on the tear-off and debonding forces, respectively. The model is made for L type composite because it causes the highest wear rate of tools. In this model, the authors attempt to use the micro-interaction to explain the high wear rates of fine-grain sintered tools in comparison with coarse-grain ones. Fig. 15 illustrates an ideal model of the whisker–tool interaction for L type composite. The following are postulated to simplify the calculation:

1. Grain boundary is supposed to be within a square shape on the rake surface as illustrated in Fig. 15(b). The edge length of the square is equal to the grain size d.
2. The tear-off planes of grains inside the tool make 45° with the force applied by whisker.
3. Tear-off modes of the grains are transverse rupture of the top plane and shear fracture in the two sides planes of the grain boundary (see Fig. 15(c)).

From Fig. 15(a) and Fig. 15(b), the required force F_r to tear off the grains of tool edge at the layer number n is given in Eq. (1). To simplify the form of the equation, it is given for rake angle = clearance angle = γ.

$$F_r = \frac{(\cos\gamma - \sin\gamma)^2}{(\cos\gamma + \sin\gamma)}(nd)^2\sigma_r + \frac{\sqrt{2}}{2}(3\cos\gamma + \sin\gamma)(\cos\gamma - \sin\gamma)(nd)^2\tau_r \quad (1)$$

where γ is the rake angle, σ_r the transverse rupture strength of tool material, n the rupture plane number, d the grain size and $\tau_r = \sigma_r/2$ the shear strength of grain boundary.

On the other hand, the maximum force F_w that should be applied by tool edge to push one whisker forward is simply given by

$$F_w = \pi DL\tau_0 + \tfrac{1}{4}\pi D^2\sigma_0 \quad (2)$$

where D is the whisker diameter, L the whisker length, τ_0 the shear debonding strength of whisker–matrix interface and σ_0 the compressive strength of the matrix.

For instance, Fig. 16 illustrates the interaction forces between the SiC whisker debonding and the tear-off of two diamond grains of tools for L type composite. The lines (No. 1) are the forces F_w that should be applied by tool edge on the end section of SiC whisker to be pushed forward with the increment of whisker diameter for lengths $L = 10, 30, 50$ μm. However, σ_0 and τ_0 are adapted to the data of tensile test of resin. The lines show the maximum possible forces when the tool edge strikes the whisker. The broken line (No. 2) shows the tear-off forces F_r of the fine grain (0.5 μm) of sintered diamond tool at the supposed fracture planes (stepped line). However, the dash-point line (No. 3) shows those of coarse grain (5 μm). In the calculation, σ_r is taken to be equal to transverse rupture strength of the tools in Table 1.

From the figure, it can be found that, at a small whisker diameter such as $D = 1$ μm, the tear-off forces of fine grain ($d = 0.5$ μm) at the first layer is close to the debonding force of whisker. When the whisker diameter is as fine as the tool grain, there is a possibility for the whisker to strike one grain individually where the tear-off force of a grain is considerably close to the debonding force of SiC whisker; hence the tear-off probability of grains of the tool edge becomes high while the tool edge is pushing the whisker forward. However, for the tool grain size ($d = 5$ μm) coarser than SiC whisker diameter (∅1 μm), even though the whisker can strike one grain individually, the tear-off force of the first layer of the coarse grain is much greater than the debonding force of SiC whisker. Hence, the tear-off rate of coarse grains is considerably lower than that of fine grains. Moreover, from lines No. 1, it can be predicted that the tear-off possibility of the diamond grains decreases with shorter whisker length since the debonding forces of whiskers decrease as well.

On the other hand, when the diameter of SiC whisker is larger than both grain sizes of tools, for instance $D = 10$ μm, the whisker can not strike one grain individually. The tear-off forces of several grains, shown in Fig. 16 at $n = 20$ for $d = 0.5$ μm and $n = 2$ for $d = 5$ μm, are much greater than the debonding force of whisker. Hence, the probability of grain

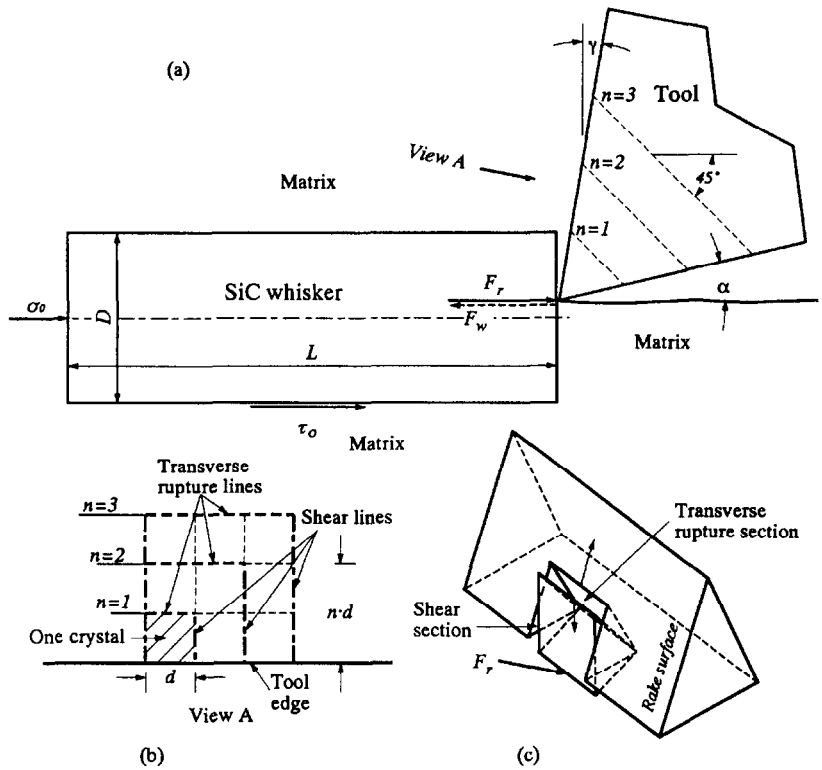

Fig. 15. Illustration of whisker–tool interaction model for L type composite: (a) SiCw–edge interaction; (b) tear-off boundaries of diamond grains; (c) grain fracture mode.

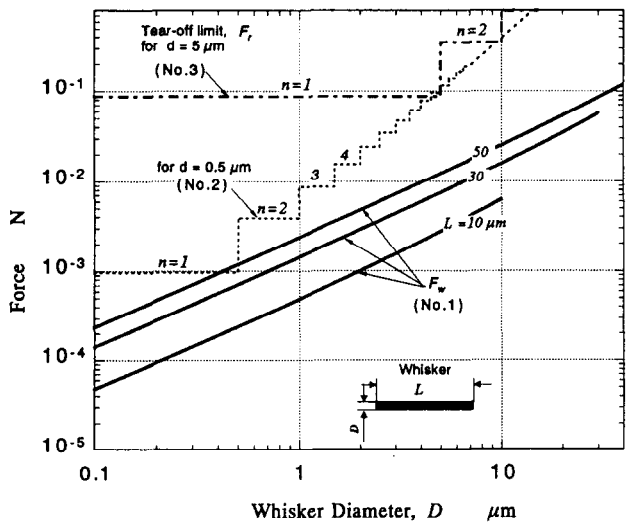

Fig. 16. Interaction forces of grain tear-off and whisker debonding in relation with whisker diameter.

tear-off decreases and the performances of both fine and coarse grain tools are supposed to be close to each other.

As a conclusion, the factor of grain size of sintered tools is involved in the wear mechanism when cutting a whisker reinforced composite if the whisker length is relatively large and its diameter is around the grain size.

5. Conclusions

In the cutting of unidirectional whisker reinforced plastic by sintered diamond tools, the following can be concluded:

1. Aligning SiC whiskers to be parallel to the cutting direction (L type composite) induced the highest wear rate in the cutting tools in comparison with N and T types in spite of the least cutting force.
2. Cutting SiC whisker–plastic composite under SEM observation demonstrates the cutting mechanisms of the composite with different whisker orientation.
3. Wear resistance of sintered diamond tool of coarse grains ($d=5$ μm) is higher than that of fine grains ($d=0.5$ μm) in cutting a SiC whisker–plastic composite with a whisker diameter of around 1 μm. A higher wear rate of a sintered diamond tool is expected when the grain size is roughly the whisker diameter.

References

[1] Y. Tsunekawa, M. Okumiya and K. Okumura, Flame-spraying fabrication of silicon carbide whisker-reinforced aluminium, *J. Mater. Sci. Lett.*, *6* (2) (1987) 191–193.

[2] K.P. Gadkaree and K. Chyung, Silicon-carbide-whisker-reinforced glass and glass–ceramic composites, *Am. Ceram. Soc. Bull.*, *65* (2) (1986) 370–376.

[3] R. Hayami et al., Si_3N_4–SiC whisker composite material, *Proc. 21st Univ. Conf. on Ceramic Science, University Park, PA, 1985*, Plenum, New York, 1986, pp. 663–674.
[4] J.R. Porter, F.F. Lange and A.H. Chokshi, Processing and creep performance of silicon carbide whisker-reinforced silicon nitride, *Advanced Structural Ceramics Symp., 1986*, Mater. Res. Soc., Swarthmore, PA, 1987, pp. 289–294.
[5] L. Bjork and A.G. Hermansson, Hot isostatically pressed alumina–silicon carbide-whisker composites, *J. Am. Ceram. Soc., 72* (8) (1989) 1436–1438.
[6] R.N. Singh, Mechanical properties of a zircon matrix composite reinforced with silicon carbide whiskers and filaments, *J. Mater. Sci., 26* (7) (1991) 1839–1846.
[7] V.C. Nardone and J.R. Strife, Analysis of the creep behavior of silicon carbide whisker reinforced 2124 Al (T4), *Metall. Trans. A, 18A* (1) (1987) 109–114.
[8] A.H. Chokshi, T.G. Nieh, J. Wadsworth and A.K. Mukherjee, The superplastic-like characteristics of a silicon carbide whisker reinforced aluminum composite, *Strength of Metals and Alloys (ICSMA 8), Proc. 8th Int. Conf., Finland, 1988*, Vol. 1, Pergamon, Oxford, 1988, pp. 301–306.
[9] R.S. Mishra and A.K. Mukherjee, On superplasticity in silicon carbide reinforced aluminum composites, *Scr. Metall. Mater., 25* (2) (1991) 271–275.
[10] Ma Zongyi et al., Abrasive wear of discontinuous SiC reinforced aluminum alloy composites, *Wear, 148*,, (2) (1991) 287–293.
[11] H. Grewe, K. Grewe and J. Kolas, Whisker-reinforced ceramics, *Ceram. Forum Int., 64* (8–9) (1987) 303, 306–308, 313–317.
[12] E.R. Billman, K. Mehrotra, A.F. Shuster and C.W. Beeghly, Machining with Al_2O_3–SiC-whisker cutting tools, *Am. Ceram. Soc. Bull., 67* (6) (1988) 1016–1019.
[13] C.S Yust, J.M. Leitnaker and C.E. Devore, Wear of an alumina–silicon carbide whisker composite, *Wear, 122* (2) (1988) 151–164.
[14] S. Iio, M. Watanabe, M. Matsubara and Y. Matsuo, Mechanical properties of alumina/silicon carbide whisker composites, *J. Am. Ceram. Soc., 72* (10) (1989) 1880–1884.
[15] G. Brandt, A. Gerendas and M. Mikus, Wear mechanisms of ceramic cutting tools when machining ferrous and non-ferrous alloys, *J. Eur. Ceram. Soc., 6* (5) (1990) 273–290.
[16] S.F. Wayne and S.-T. Buljan, Wear of ceramic cutting tools in Ni-based superalloy machining, *Tribol. Trans., 33* (4) (1990) 618–626.
[17] R. Hayami, M. Kinoshita, K. Ueno and T. Yamamoto, Cutting tool of SiC whisker/alumina ceramic composite, in *Advanced Structural Inorganic Composite, Proc. 7th CIMTEC—World Ceramics Congr., Italy, 1990*, Elsevier, Amsterdam, 1991, pp. 453–458.
[18] S. Lo Casto et al., Wear performance of ceramic cutting tool materials when cutting steel, *Proc. 7th Int. Conf. on Computer-Aided Production Engineering, USA*, Elsevier, Amsterdam, 1991, pp. 25–36.
[19] A.R. Thangaraj and K.J. Weinmann, On the wear mechanisms and cutting performance of silicon carbide whisker-reinforced alumina, *J. Eng. Ind. (Trans. ASME), 114* (1992) 301–307.
[20] X.S. Li and M. Low, Evaluation of advanced alumina-based ceramic tool inserts when machining high-tensile steel, *J. Mater. Sci., 29* (12) (1994) 3121–3127.
[21] H. Xiao, X. Ai and H.S. Yang, Effect of whisker orientation on the wear behavior of a SiC/Al_2O_3 composite, *Wear 148* (1) (1991) 171–180.
[22] H. Xiao, X. Ai and H.S. Yang, Effect of whisker orientation on toughening behavior and cutting performance of $SiCw–Al_2O_3$ composites, *Mater. Sci. Technol., 9* (1) (1993) 21–25.
[23] Y. Zhang, C.A Pickles and J. Cameron, The production and mechanical properties of SiC whisker-reinforced epoxy composites, *J. Reinforced Plastics and Composites, 11* (1992) 1176–1186.
[24] J. Shyne and R.G. Shaver, *Whisker Composite Technologies*, SAMPLE, San Diego, CA, 1966.
[25] K. Yamaguchi and I. Horaguchi, Development of directionally aligned SiC whisker wheel, *Precis. Eng., 17* (1) (1995) 5–9.